

# Solid-state NMR spectroscopy of roasted and ground coffee samples: evidences for phase heterogeneity and prospects of applications in food screening

Jair C. C. Freitas<sup>1,2\*</sup>, Maryam Ejaz<sup>2</sup>, Aline T. Toci<sup>3</sup>, Wanderson Romão<sup>4,5</sup>, Yaroslav Z. Khimyak<sup>2\*</sup>

<sup>1</sup>Laboratory of Carbon and Ceramic Materials, Department of Physics, Federal University of Espírito Santo (UFES), Av. Fernando Ferrari, 514, 29075-910, Vitória, ES, Brazil

<sup>2</sup>School of Pharmacy, University of East Anglia, Norwich Research Park, Norwich NR4 7TJ, UK

<sup>3</sup>Environmental and Food Interdisciplinary Studies Laboratory (LEIMAA), Latin American Institute of Life and Nature Science, Federal University for Latin American Integration (UNILA), 85867-970, Foz do Iguaçu, PR, Brazil

<sup>4</sup>Laboratory of Petroleomics and Forensics, Federal University of Espírito Santo (UFES), Av. Fernando Ferrari, 514, 29075-910, Vitória, ES, Brazil

<sup>5</sup>Federal Institute of Espírito Santo (IFES), Av. Ministro Salgado Filho, 29106-010, Vila Velha, ES, Brazil

**Abstract** – The advancement in the use of spectroscopic techniques to investigate coffee samples is of high interest especially considering the widespread problems with coffee adulteration and counterfeiting. In this work, the use of solid-state nuclear magnetic resonance (NMR) is investigated as a means to probe the various chemically-distinct phases existent in roasted coffee samples and to detect the occurrence of counterfeiting or adulterations in coffee blends. Routine solid-state <sup>1</sup>H and <sup>13</sup>C NMR spectra allowed the distinction between different coffee types (Arabica / Robusta) and the evaluation of the presence of these components in coffee blends. On the other hand, the use of more specialized solid-state NMR experiments revealed the existence of phases with different molecular mobilities (e.g., associated with lipids or carbohydrates). The results illustrate the usefulness of solid-state NMR spectroscopy to examine molecular mobilities and interactions and to aid in the quality control of coffee-related products.

**Keywords** – Solid-state NMR; Roasted and ground coffee; Food composition; Adulteration.

---

\* Corresponding authors. E-mail addresses: [jairccfreitas@yahoo.com.br](mailto:jairccfreitas@yahoo.com.br) (JCCF), [y.khimyak@uea.ac.uk](mailto:y.khimyak@uea.ac.uk) (YZK).

## 25 **1. Introduction**

26 Coffee is one of the most sought-after commodities in the world (International Coffee  
27 Organization, 2021). As such, there is a huge interest in the development of efficient methods that  
28 can be successfully employed for screening and quality control of coffee beans and coffee-derived  
29 products. The deep understanding about the chemical composition of coffee is relevant not only from  
30 the food science point of view, but also due to the pharmacological relevance of many of its  
31 components (e.g., caffeine, chlorogenic acids and diterpenes) (Esquivel & Jiménez, 2012; Cano-  
32 Marquina, Tarín, & Cano, 2013). There are two commercially relevant coffee species, *Coffea arabica*  
33 (known as Arabica coffee) and *C. canephora* (known as Robusta or Conilon coffee) (Finotello,  
34 Forzato, Gasparini, Mammi, Navarini, & Schievano, 2017). Beverages obtained from Arabica coffee  
35 generally exhibit richer taste and aroma as compared to Robusta, which means that Arabica coffee  
36 has a higher value in the market than the Robusta form. Therefore, adulteration of the more expensive  
37 form with the cheaper one can lead to fraudulent commercial gain. In contrast with intact coffee  
38 beans, it is more difficult to find out the authenticity of ground roasted coffee upon inspection.  
39 Therefore, it is highly desirable to establish efficient tools that can allow the detection and  
40 quantification of the presence of Robusta coffee in commercial products labelled as “100 % Arabica”.  
41 Many efforts have been taken in this way, involving the use of spectroscopic methods – e.g., mass  
42 spectrometry, liquid chromatography, ultraviolet-visible (UV-Vis), Fourier-transform infrared  
43 (FTIR), near infrared (NIR) and solution <sup>1</sup>H nuclear magnetic resonance (NMR) spectroscopies – to  
44 discriminate Arabica and Robusta varieties in both raw and ground roasted coffee samples (Kemsley,  
45 Ruault, & Wilson, 1995; Monakhova et al., 2015; Defernez et al., 2017; Hong et al., 2017; Correia et  
46 al., 2018; Gunning et al., 2018). Furthermore, methods as these have also been applied aiming the  
47 detection of several types of adulterants fraudulently mixed with roasted coffee (again to obtain  
48 cheaper mixtures), such as corn, barley, rice, soybean, wheat, chickpea and coffee husks (Toci, Farah,  
49 Pezza, & Pezza, 2016; Hong et al., 2017; Ribeiro, Boralle, Pezza, Pezza, & Toci, 2017; Sezer,  
50 Apaydin, Bilge, & Boyaci, 2018; Milani, Rossini, Catelani, Pezza, Toci, & Pezza, 2020).

51 Solution  $^1\text{H}$  and  $^{13}\text{C}$  NMR spectroscopy has been used as a screening protocol in many studies of  
52 coffee products, including raw and roasted coffee beans (Bosco, Toffanin, De Palo, Zatti, & Segre,  
53 1999; Wei et al., 2012; Monakhova et al., 2015; Defernez et al., 2017; Finotello et al., 2017; Ribeiro  
54 et al., 2017; Hong et al., 2017; Gunning et al., 2018; Milani et al., 2020). The main benefits of NMR  
55 spectroscopy in comparison with other spectroscopic methods include the ease of sample preparation  
56 (with no need of time-consuming purification or chemical derivation stages), the quantitative  
57 character of the technique and the high resolution of the NMR spectra that allow the identification of  
58 the components present in the solution (Bosco et al., 1999; Wei et al., 2012). Solid-state NMR spectra  
59 have inferior resolution in comparison with spectra recorded in solution, so the applicability of solid-  
60 state NMR spectroscopy to studies involving coffee samples is somewhat limited. Nevertheless, some  
61 examples can be found in the literature where solid-state NMR spectra have been exploited to obtain  
62 information on chemical aspects of coffee beans and other coffee-related materials (Nogueira, Boffo,  
63 Tavares, Moreira, Tavares, & Ferreira, 2011; Low, Rahman, & Jamaluddin, 2015; Kanai, Yoshihara,  
64 & Kawamura, 2019). For instance, a recent report has described the use of solid-state  $^1\text{H}$  and  $^{13}\text{C}$   
65 NMR spectra to assess the contributions due to lipids and polysaccharides in raw coffee beans, roasted  
66 coffee beans and spent coffee grounds, noting that these lipids are a potential source for the production  
67 of biofuels (Kanai et al., 2019). The most outstanding advantage of solid-state NMR in comparison  
68 with solution NMR experiments refers to the possibility of conducting the experiments with  
69 essentially no sample preparation or modification; the material to be analysed (e.g., raw coffee beans,  
70 roasted coffee beans or granules and spent coffee grounds) can be directly powdered and packed into  
71 the NMR rotor, so as to obtain spectra representative of the intact sample. In this regard, the  
72 development of solid-state NMR spectroscopy methods that can be used in studies of intact coffee  
73 products is of high interest.

74 In this work, the use of solid-state NMR spectroscopy is exploited in detail to study roasted coffee  
75 samples, with special emphasis on the assessment of the chemically heterogeneous nature of products  
76 of the Arabica and Robusta variants. The main hypothesis to be examined here is that solid-state

77 NMR spectroscopy can be used effectively to assess the chemical composition of roasted coffee  
78 samples, without any chemical modifications, and are also useful for screening purposes to detect  
79 counterfeiting of coffee products. Whereas many previous NMR studies dealing with coffee products  
80 have been conducted in solution (with the extraction of hydrophilic or lipophilic components of  
81 coffee), the present investigation involves solid-state NMR experiments conducted with intact roasted  
82 and ground coffee samples. With the use of pulse sequences suitable to emphasize the different  
83 responses of phases with distinct dynamics present in the material, the contributions due to lipids and  
84 carbohydrates are identified in  $^1\text{H}$  and  $^{13}\text{C}$  NMR experiments carried out with intact samples. As  
85 detailed later, the identification of the signals due to lipids is particularly important for authentication  
86 purposes, since Arabica and Robusta varieties exhibit different amounts of lipids and also distinct  
87 types of diterpenes present in the lipid fraction. The solid-state NMR experiments are non-destructive,  
88 relatively fast and straightforward to implement in commercial NMR spectrometers equipped with  
89 conventional solid-state probes. Moreover, the potential of solid-state NMR spectroscopy to allow  
90 the distinction of the contributions from Arabica and Robusta coffee variants in coffee blends is also  
91 demonstrated, illustrating the usefulness of this approach for screening and identification of  
92 counterfeit coffee products.

93

## 94 **2. Experimental methods**

### 95 *2.1 Samples*

96 Samples of Arabica and Robusta ground roasted coffee beans were obtained from the state Minas  
97 Gerais (MG), in southeast Brazil. From these samples, seven mixtures were prepared with differing  
98 amounts of Arabica and Robusta coffee variants (i.e., with 0, 5, 25, 50, 75, 95, and 100 wt. % of  
99 Arabica coffee in the mixture). The coffee samples were gently ground using a mortar and pestle into  
100 a fine and homogenous powder, which was packed into a 4 mm NMR rotor; the mass of sample inside  
101 the rotor was in the range 50-60 mg.

102

## 103 2.2 NMR experiments

104 Solid-state NMR experiments were conducted at room temperature in a 300 MHz Bruker Avance  
105 spectrometer III running the Topspin 3.2 software. The powdered coffee samples were packed into  
106 4 mm diameter zirconia rotors for magic angle spinning (MAS) experiments at the frequency of  
107 12 kHz. Both  $^1\text{H}$  and  $^{13}\text{C}$  NMR experiments were conducted, at frequencies of 300.13 and  
108 75.47 MHz, respectively. The one-dimensional (1D) spectra were obtained by Fourier transform of  
109 the free induction decays (FIDs), after zero filling (twice) and exponential line broadening of 1 and  
110 50 Hz for  $^1\text{H}$  and  $^{13}\text{C}$  NMR spectra, respectively. The chemical shifts were expressed in parts per  
111 million (ppm) and were referenced to tetramethylsilane (TMS), using adamantane and  
112 hexamethylbenzene (HMB) as secondary references for  $^1\text{H}$  and  $^{13}\text{C}$  NMR spectra, respectively.  
113 Different sets of experiments were conducted for each probe nucleus, as described in the sequence.

114 The  $^1\text{H}$  NMR spectra were recorded using single pulse (SP) excitation, with a  $\pi/2$  pulse duration of  
115 3.5  $\mu\text{s}$ , a recycle delay of 5 s, a spectral window of 12 kHz (or 100 kHz in some cases, to allow the  
116 recording of the spinning sidebands) and the accumulation of 256 scans. In order to suppress the  
117 contribution from rigid components with short transverse relaxation time ( $T_2$ ), which are responsible  
118 for the production of strong and broad resonances affecting the baseline underneath the narrow signals  
119 due to the more mobile components, a “ $T_2$  filter” was included before the  $\pi/2$  excitation pulse,  
120 composed by the block of pulses:  $(\pi/2)_x - \tau - (\pi)_y - \tau$  (Mackenzie & Smith, 2002; Rastrelli, Jha, &  
121 Mancin, 2009). The time delay  $\tau$  was set at 1 ms, after several tests conducted to reach a compromise  
122 between the suppression of the broad contributions and the overall signal loss due to transverse  
123 relaxation. The longitudinal relaxation time ( $T_1$ ) was measured selectively for the mobile components  
124 by inserting the following block of pulses after the  $T_2$  filter and just before the  $\pi/2$  excitation pulse:  
125  $(\pi/2)_{\pm x} - t_{\text{REC}} - (\pi/2)_{\mp x}$ . This type of block pulse is commonly used to study spin diffusion in polymers  
126 and other materials (Kumashiro, Schmidt-Rohr, Murphy, Ouellette, Cramer, & Thompson, 1998); the

127 first  $\pi/2$  pulse in the block transfers the nuclear magnetization (which survived after the  $T_2$  filter) to  
128 the  $z$  axis; after the recovery time ( $t_{\text{REC}}$ ), the magnetization is transferred back to the transverse plane  
129 by the second  $\pi/2$  pulse (with inverted phase), for detection. In the absence of spin diffusion (which  
130 was not significant in the experiments involving the coffee samples studied here, as described later),  
131 the detected signal is attenuated only by longitudinal relaxation occurring during the interval  $t_{\text{REC}}$ .  
132 Thus, this method allows the selective study of the longitudinal relaxation process of the mobile  
133 components present in the material.

134 As for the  $^{13}\text{C}$  nuclei, the  $^1\text{H}$ - $^{13}\text{C}$  cross polarization (CP) experiments comprised the use of a  $\pi/2$   $^1\text{H}$   
135 excitation pulse of  $3.5\ \mu\text{s}$ , a contact time of  $1000\ \mu\text{s}$  (chosen after optimization of the overall signal  
136 intensity), a recycle delay of  $5\ \text{s}$ , a spectral window of  $50\ \text{kHz}$  and the accumulation of  $1024$  scans.  
137 A linear (“ramped”) variation of the RF amplitude was included in the  $^1\text{H}$  channel during the contact  
138 time and high-power  $^1\text{H}$  decoupling with small phase incremental alteration in  $64$  steps (SPINAL-64)  
139 was employed during the FID detection. In order to investigate the contributions of species with  
140 distinct molecular mobilities to the  $^{13}\text{C}$  NMR spectra, experiments combining cross polarization and  
141 single pulse excitation (known as CP-SP experiments) were also conducted (Shu, Li, Chen, & Zhang,  
142 2010). In these experiments, a  $\pi/2$   $^{13}\text{C}$  excitation pulse of  $4.5\ \mu\text{s}$  was added just before the contact  
143 time. The spectra recorded in the CP-SP experiments are expected to contain contributions from both  
144 the rigid and the mobile components, whereas the CP spectra typically contain just the contributions  
145 from the rigid components, since molecular motion averages out the dipolar coupling between the  $^1\text{H}$   
146 and  $^{13}\text{C}$  nuclei (Shu et al., 2010; Courtier-Murias et al., 2014). This selectivity of the CP process  
147 towards the rigid components also allowed the indirect measurement of the  $T_1$  values for the  $^1\text{H}$  nuclei  
148 in these moieties; for this, a saturation-recovery experiment was conducted by inserting a saturation  
149 train containing  $4$   $\pi/2$  pulses separated by  $1\ \text{ms}$  in the  $^1\text{H}$  channel, followed by variable recovery  
150 intervals, prior to the polarization transfer to the  $^{13}\text{C}$  nuclei.

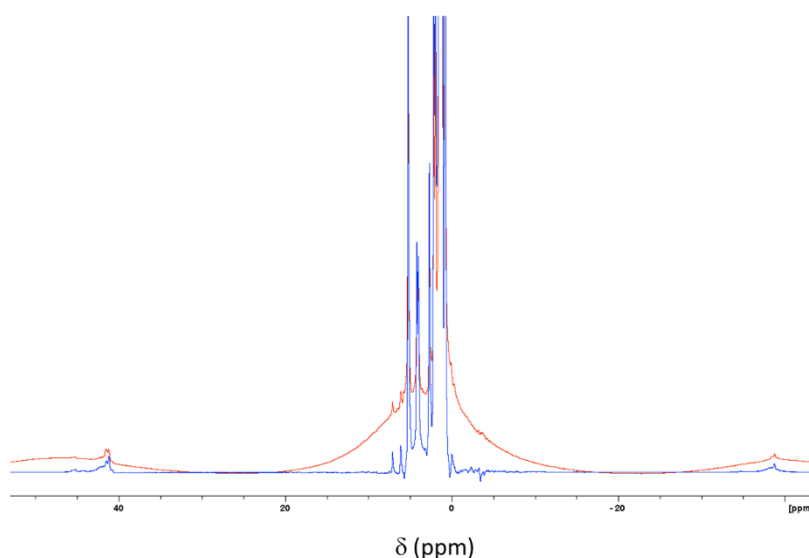
151 Two-dimensional (2D)  $^1\text{H}$ - $^{13}\text{C}$  CP-based wideline separation (WISE) experiments were also  
152 performed, in order to investigate the correlation between  $^1\text{H}$  NMR signals due to groups with  
153 different molecular mobilities and chemically distinct  $^{13}\text{C}$  resonances (Schmidt-Rohr et al., 1992).  
154 The same values of contact time,  $^1\text{H}$  excitation pulse length and recycle delays used in the 1D CP  
155 experiments were also used in the 2D WISE experiments. The spectral window in the indirect  
156 dimension ( $F_1$ ) was 100 kHz, with a total of 128 increments of the evolution time ( $t_1$ ) and  
157 accumulation of 128 scans for each  $t_1$  value.

158

### 159 **3. Results and discussion**

160 Typical  $^1\text{H}$  MAS NMR spectra obtained for a ground coffee sample (containing 100 wt. % Arabica  
161 coffee) are shown in Fig. 1. These spectra were recorded with a large spectral window (100 kHz), so  
162 that first-order spinning sidebands are clearly identified. The spectrum recorded with a conventional  
163 single pulse excitation experiment (shown in red) contains contributions from both the rigid and the  
164 mobile components; the rigid components (mostly corresponding to carbohydrates) give rise to  
165 extremely broad resonances, including the centerband and the spinning sidebands. For these  
166 components, the MAS rate used in the NMR experiments (12 kHz) is not sufficiently high to suppress  
167 the strong  $^1\text{H}$ - $^1\text{H}$  dipolar couplings, leading to the observation of a considerable homogeneous  
168 broadening that limits the overall spectral resolution. Such broad contributions appear in the  $^1\text{H}$  NMR  
169 spectrum as a featureless background, on the top of which the narrow signals due to the mobile  
170 components (associated with lipids) appear. It is worth noting that spinning sidebands are also  
171 observed for these narrow signals, indicating that the removal of the anisotropic broadening by  
172 molecular motion is just partial and so these components cannot be considered “liquid-like”, as it has  
173 been suggested in previous investigations dealing with raw and roasted coffee beans (Kanai et al.,  
174 2019).

175 Also, in the work by Kanai et al. (2019), a broad component centered around 4.5 ppm in the  $^1\text{H}$  NMR  
176 spectra of raw and roasted coffee beans has been attributed to the occurrence of water molecules with  
177 limited mobility. The broad signals observed in the present study in the spectra recorded with a  
178 conventional single pulse excitation experiment (shown in red in Fig. 1) also have the centerband  
179 occurring at similar chemical shifts; however, the origin of these broad signals is unambiguously  
180 identified as related to carbohydrates, as it will become clear in the discussion of the 2D  $^1\text{H}$ - $^{13}\text{C}$  CP-  
181 based WISE spectra (see below).



182

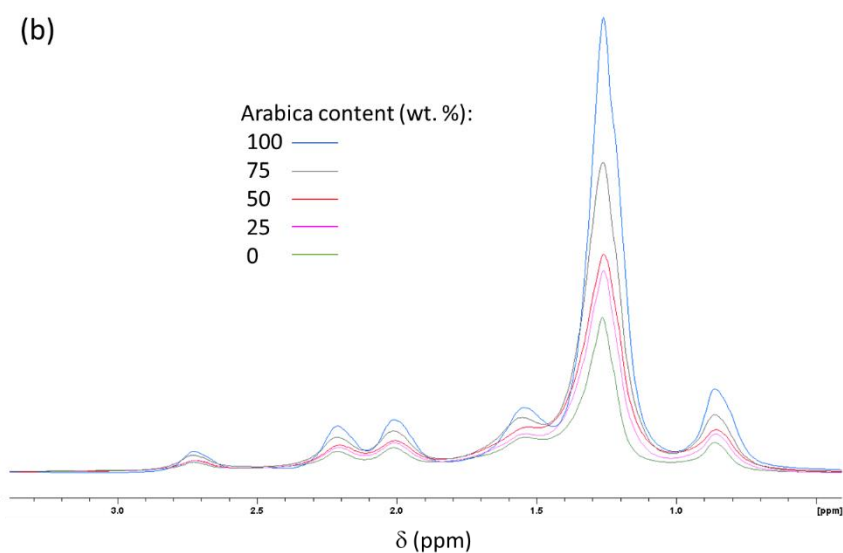
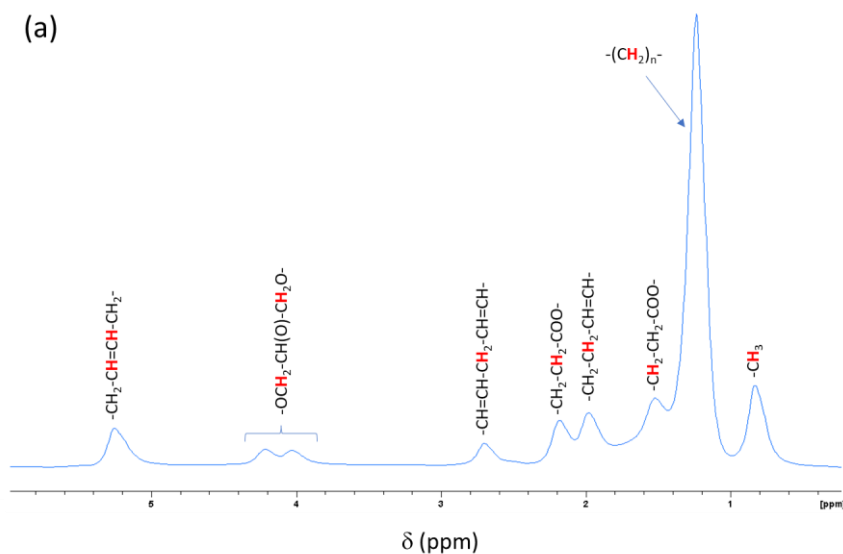
183 **Figure 1** –  $^1\text{H}$  MAS NMR spectra recorded for the sample containing 100 wt. % Arabica coffee and  
184 exhibited in a wide spectral range, including (blue line) or not (red line) the  $T_2$  filter before the  $\pi/2$   
185 excitation pulse.

186

187 With the use of the  $T_2$  filter, the contributions due to the mobile components in the  $^1\text{H}$  NMR spectra  
188 of the coffee samples are observed with a remarkably improved resolution, as illustrated in Fig. 2.  
189 This high resolution is not usual for  $^1\text{H}$  NMR spectra recorded at moderate MAS rates in solid samples  
190 with no homonuclear decoupling scheme (Lesage, 2009), but similar spectra have been previously  
191 reported for raw and roasted coffee beans (Nogueira et al., 2011; Kanai et al., 2019). As mentioned  
192 above, the observation of these narrow lines is a direct indication of the highly mobile character of

193 the lipid molecules present in the coffee samples. It is worth noting that Kanai et al. (2019) reported  
194 the detection of  $^1\text{H}$  NMR spectra containing only the narrow contributions for the liquid lipid residue  
195 obtained after extraction with *n*-hexane, which was obviously free of carbohydrate contributions. In  
196 the present work, the use of the  $T_2$  filter led to the achievement of  $^1\text{H}$  NMR spectra containing just  
197 the lipid contributions in a straightforward way, which thus allows the possibility of obtaining detailed  
198 chemical information about these moieties without the need of laborious extraction methods.

199 The  $^1\text{H}$  NMR spectra shown in Fig. 2 are representative of the triacylglycerides (TAGs) present in  
200 coffee. The detected signals are similar to the ones present in  $^1\text{H}$  NMR spectra recorded in solution  
201 for several types of edible oils, due to the structural resemblance of the fatty acids present in coffee  
202 and in other sources such as corn, olive and hazelnut oils (D'Amelio, De Angelis, Navarini,  
203 Schievano, & Mammi, 2013; Parker, Limer, Watson, Defernez, Williamson, & Kemsley, 2014). A  
204 detailed assignment of the chemical shifts identified in the  $^1\text{H}$  NMR spectra of coffee samples has  
205 been provided before, indicating that the TAGs present in coffee involve mixtures mostly containing  
206 saturated fatty acids, oleic and linoleic acids (D'Amelio et al, 2013; Kanai et al., 2019). The dominant  
207 peak in these spectra occurs at 1.3 ppm, due to chain methylene groups, whereas other easily  
208 identifiable signals include terminal methyl, allylic, bis-allylic, glyceride and olefinic groups (see Fig.  
209 2a).



210

211

212 **Figure 2** –  $^1\text{H}$  MAS NMR spectrum recorded with the  $T_2$  filter before the  $\pi/2$  excitation pulse for the  
 213 sample containing 100 wt. % Arabica coffee, with indication of the chemical groups responsible for  
 214 the dominant signals (a), and for a set of samples containing mixtures of Arabica and Robusta coffee  
 215 in different proportions (b).

216

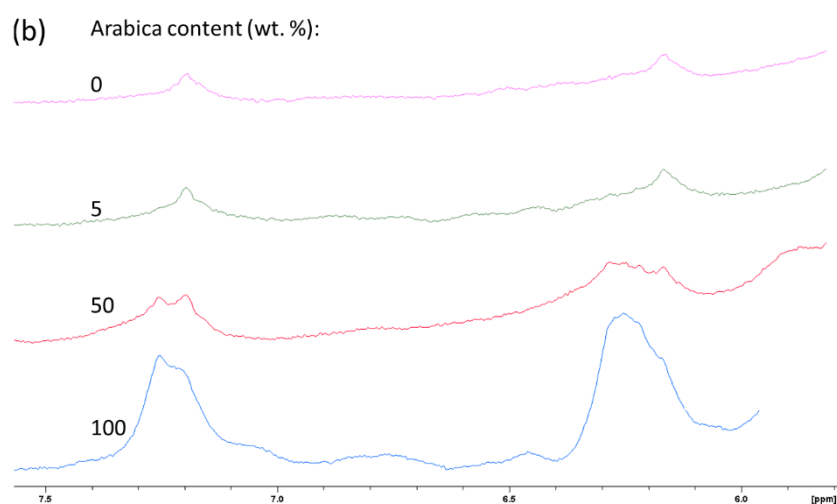
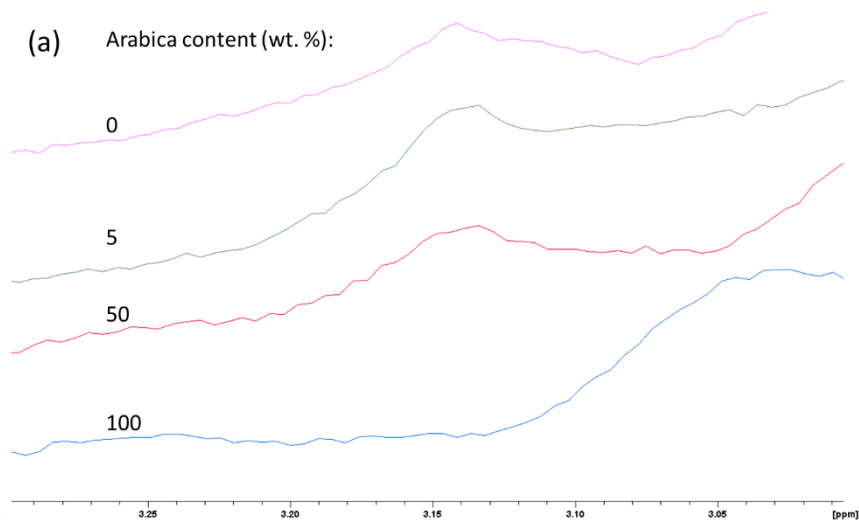
217 All these resonances are common for the TAGs present in both types of coffee analysed in this work;  
 218 the main differences between the Arabica and Robusta varieties in this regard correspond to the  
 219 amount of lipids, which is considerably higher in Arabica coffee (Speer & Kölling-Speer, 2006;

220 D'Amelio et al, 2013). Consequently, the absolute intensity of the narrow signals in the  $^1\text{H}$  NMR  
221 spectra obtained for the coffee mixtures (after correcting for the different sample masses used in each  
222 experiment) shows a steady increase as a function of the Arabica content in the mixture, as illustrated  
223 for a representative set of samples in Fig. 2b. It is worth noting that these spectra were recorded using  
224 exactly the same experimental conditions and the intensities were normalized by the sample masses,  
225 so that the absolute intensities can be reliably compared from sample to sample. The quantitative  
226 character of this comparative analysis could be improved by using an internal reference standard (with  
227 a reference peak with known intensity) or an electronically-synthesized reference signal, as  
228 commonly done in quantitative NMR (Bharti & Roy, 2012). But, even without these procedures, the  
229 results shown in Fig. 2b clearly demonstrate how the distinct lipid contents of Arabica and Robusta  
230 coffee lead to significant differences in the strong peaks present in the solid-state  $^1\text{H}$  NMR spectra  
231 recorded with the  $T_2$  filter.

232 On the other hand, there are some less intense signals obtained in solid-state  $^1\text{H}$  NMR experiments  
233 that can be used to distinguish the Arabica and Robusta varieties, due to the differences in the  
234 chemical composition of the lipids. In fact, the signals associated with coffee diterpenes such as  
235 kahweol, cafestol and 16-O-methylcafestol (16-OMC) have been used in previous solution NMR  
236 investigations as indicators of the presence of Arabica or Robusta varieties and thus are useful for  
237 studies aiming authenticity checks of coffee mixtures (Monakhova et al., 2015; Defernez et al., 2017;  
238 Finotello et al., 2017; Gunning et al., 2018). Among these, kahweol is known to be present mostly in  
239 Arabica forms and is less common in Robusta, whereas cafestol is common in both varieties. On the  
240 other hand, 16-OMC has long been thought to occur only in Robusta coffee and thus considered as a  
241 useful marker for coffee authenticity, also because this compound is stable during the roasting process  
242 (Speer & Kölling-Speer, 2006; D'Amelio et al, 2013; Defernez et al., 2017). However, a recent work  
243 has disputed this consensus by claiming that 16-OMC is also present in Arabica, albeit in very small  
244 amounts (Gunning et al., 2018). All these diterpenes produce signals that can be easily identified in  
245 high-resolution  $^1\text{H}$  NMR spectra of lipophilic coffee extracts (D'Amelio et al, 2013; Monakhova et

246 al., 2015), even at low magnetic fields (Defernez et al., 2017). Specific signals due to kahweol and  
247 cafestol appear in the range 5.9-7.3 ppm, whereas 16-OMC gives rise to a well-defined signal around  
248 3.16 ppm in solution  $^1\text{H}$  NMR spectra obtained for coffee oil and lipophilic coffee extracts (D'Amelio  
249 et al., 2013; Defernez et al., 2017).

250 The possibility of detection of the signals due to kahweol, cafestol and 16-OMC in solid-state  $^1\text{H}$   
251 NMR spectra of roasted coffee samples is demonstrated in Fig. 3, taking advantage of the significant  
252 improvement in resolution obtained due to the use of the  $T_2$  filter. Clear differences are observed  
253 between the signals observed for pure Arabica and pure Robusta; moreover, a progressive change in  
254 these signals is observed for the mixtures containing different amounts of each coffee variety. The  
255 peak around 3.15 ppm (due to methyl groups in 16-OMC) shows a steady growth with the increase  
256 in the amount of Robusta coffee in the mixtures. On the other hand, the resonances between 6.0 and  
257 7.5 ppm are significantly more intense for the samples containing more amount of Arabica coffee,  
258 which is consistent with the higher oil content of these samples (see also Fig. 2b); the number of  
259 signals detected in this range and their chemical shifts also show a continuous change with the  
260 increase in the Arabica coffee amount in the mixtures, which is a direct consequence of the differences  
261 in diterpene composition of Robusta and Arabica coffee varieties (Speer & Kölling-Speer, 2006;  
262 D'Amelio et al, 2013; Defernez et al., 2017). Thus, since the solid-state  $^1\text{H}$  NMR spectra of coffee  
263 samples are completely dominated by the contribution due to coffee oil and considering that the main  
264 signals useful to differentiate Arabica and Robusta varieties are due to the diterpenes present in the  
265 lipid fraction, this method can indeed be useful for screening studies aiming to assess the authenticity  
266 of coffee products. This could be facilitated using chemometric multivariate methods, similarly to  
267 what has been done using solution-state NMR experiments with lipophilic coffee extracts (Defernez  
268 et al., 2017; Gunning et al., 2018).



269

270

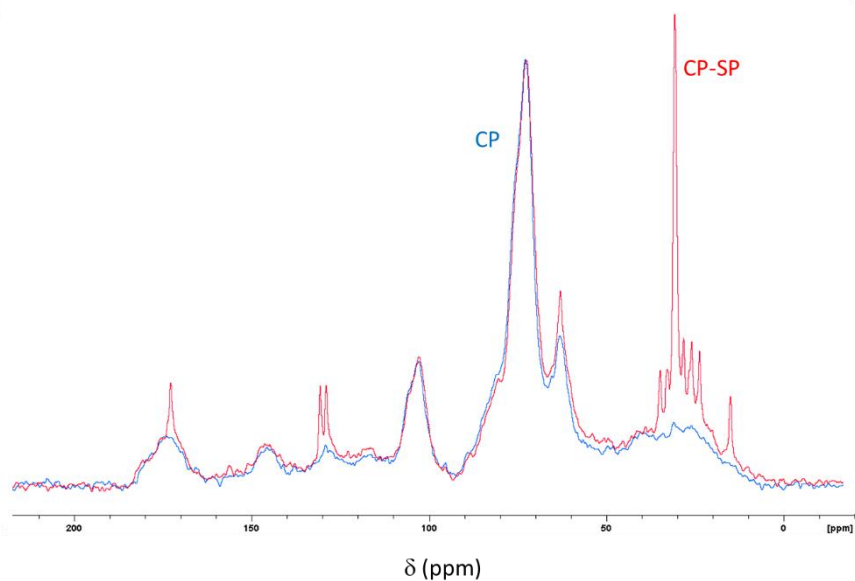
271 **Figure 3** –  $^1\text{H}$  MAS NMR spectra recorded with the  $T_2$  filter before the  $\pi/2$  excitation pulse for a set  
 272 of samples containing mixtures of Arabica and Robusta coffee in different proportions, highlighting  
 273 the chemical shift ranges containing typical signals due to diterpenes 16-OMC (a), cafestol and  
 274 kahweol (b).

275

276 It is worth stressing at this point some important advantages of solid-state  $^1\text{H}$  NMR spectroscopy  
277 regarding the possibility of identification of the signals due to 16-OMC for coffee authenticity  
278 applications. First of all, there is the obvious practical benefit of analyzing the coffee samples as  
279 received, with no need to dilute or obtain lipophilic extracts (as required in solution NMR  
280 experiments). Furthermore, several previous works have documented that the 16-OMC compound is  
281 not stable in chloroform solutions, especially when exposed to light, and thus the solution  $^1\text{H}$  NMR  
282 spectra need to be recorded ideally within hours after extraction (D'Amelio et al., 2013; Defernez et  
283 al., 2017). In the case of  $^1\text{H}$  solid-state NMR experiments reported here, no extraction is required and  
284 the presence of the 16-OMC marker can be analysed without destroying the structure of the coffee  
285 beans / powders, with no need to protect the sample to avoid degradation. The  $^1\text{H}$  NMR spectra shown  
286 in Fig. 3 are fully reproducible and do not change over time, which is a huge advantage from the  
287 practical point of view.

288 The coexistence of phases with markedly different mobilities can also be assessed by solid-state  $^{13}\text{C}$   
289 NMR spectroscopy. As mentioned before, the  $^{13}\text{C}$  NMR spectra of coffee samples obtained with CP  
290 are expected to be dominated by signals due to rigid components in carbohydrates, whereas the mobile  
291 components (in lipids) should contribute preferentially to the CP-SP spectra (Shu et al., 2010;  
292 Courtier-Murias et al., 2014). These features are clearly observed in the comparison shown in Figure  
293 4, where the  $^{13}\text{C}$  CP and CP-SP MAS NMR spectra are compared for the pure Arabica coffee sample;  
294 similar findings were also observed for the other coffee samples. In these spectra, the somewhat broad  
295 signals around 66, 74, 105 and 172 ppm are due to carbohydrates (mostly cellulose and  
296 hemicellulose), as it is commonly found in many different types of lignocellulosic materials  
297 (Cipriano, Chinelatto Jr., Nascimento, Rezende, de Menezes, & Freitas, 2020). In the case of coffee,  
298 these carbohydrates constitute the fibers present in the cell walls in the coffee beans (Kanai et al.,  
299 2019; Kanai et al., 2020).

300



301

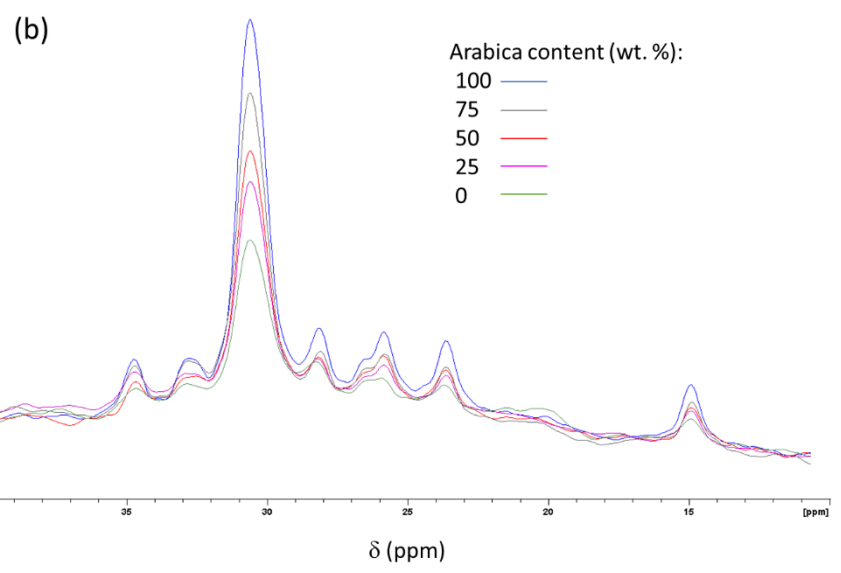
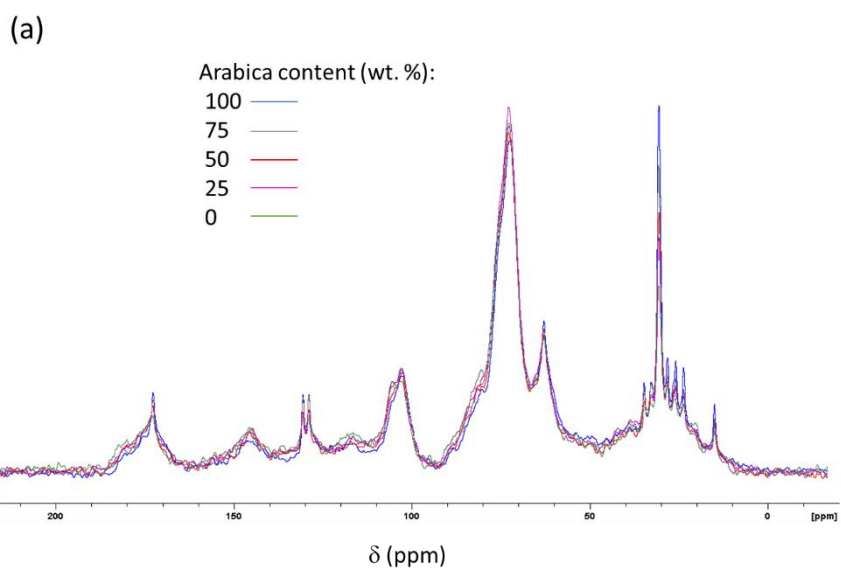
302 **Figure 4** – Comparison of  $^{13}\text{C}$  CP (blue line) and CP-SP (red line) MAS NMR spectra recorded for  
 303 the sample containing 100 wt. % Arabica coffee.

304

305 Besides these resonances, the  $^{13}\text{C}$  CP-SP MAS NMR spectra (Fig. 4) also contain a number of narrow  
 306 peaks, similar to the ones observed in the  $^1\text{H}$  MAS NMR spectra (Fig. 2). These lines are once more  
 307 ascribed to the lipid moieties, which exhibit large molecular mobility and thus are unable to produce  
 308 efficient  $^1\text{H}$ - $^{13}\text{C}$  polarization transfer, making impossible their full observation in the CP spectra. The  
 309 chemical shifts of the narrow signals are consistent with previous results obtained for oils derived  
 310 from coffee and other sources, showing the occurrence of TAGs composed of mixtures of saturated  
 311 fatty acids, oleic and linoleic acids (D'Amelio et al., 2013; Kanai et al., 2019). The most intense  
 312 narrow peaks in the CP-SP spectra are observed in the range 10-40 ppm, due to aliphatic  $\text{CH}_3$  and  
 313  $\text{CH}_2$  groups in the fatty acid chains (with the strongest  $\text{CH}_2$  peak appearing at 32 ppm); other narrow  
 314 peaks appear around 63 ppm (O-alkyl groups), 125 and 128 ppm (olefinic carbons), and 172 ppm  
 315 (ester carbonyl groups).

316 The relative intensities of these narrow peaks in the CP-SP spectra show a steady growth with the  
317 increase in the amount of Arabica coffee in the mixtures, as shown in Fig. 5, which is obviously a  
318 consequence of the larger oil concentration in Arabica coffee in comparison with the Robusta variety.  
319 This type of correlation points thus to another possibility (now using solid-state  $^{13}\text{C}$  CP-SP MAS  
320 NMR experiments) for the development of quantitative methods to determine the amount of Arabica  
321 coffee in blends, which should be explored in future investigations.

322 The heterogeneous character of the coffee samples investigated in this work can be further assessed  
323 using solid-state NMR experiments sensitive to the dynamic aspects related to each phase present in  
324 the material. First, spin-lattice relaxation time measurements are a useful tool to probe the space  
325 proximity between chemical groups belonging to phases with different mobilities. Due to the process  
326 of spin diffusion mediated by the homonuclear dipolar coupling between  $^1\text{H}$  nuclei, the corresponding  
327  $T_1$  values associated with spatially close spins in rigid domains tend to become the same; for organic  
328 materials, the domain size corresponding to a uniform  $T_1$  value has been estimated in the range of  
329 tens of nanometers (Aso et al., 2007). On the other hand, systems exhibiting phase separation (i.e.,  
330 with domain sizes above this range) are expected to display distinct  $^1\text{H}$   $T_1$  values corresponding to  
331 each phase (when these values are distinct for the pure phases). Approaches based on relaxation time  
332 and/or spin diffusion measurements have long been used to study phase separation and to estimate  
333 domain sizes in polymer blends, pharmaceutical dispersions and biological systems, among others  
334 (Clauss, Schmidt-Rohr, & Spiess, 1993; Duan et al., 2020).



335

336

337 **Figure 5** –  $^{13}\text{C}$  CP-SP MAS NMR spectra recorded for a set of samples containing mixtures of  
 338 Arabica and Robusta coffee in different proportions, shown in full range (a) and in the spectral range  
 339 corresponding to the lipid signals (b).

340

341 In the case of the coffee samples described here, the  $^1\text{H}$   $T_1$  values were measured separately for the  
 342 mobile and rigid components for a representative sample (containing 100 wt. % Arabica coffee),  
 343 using the methods described in Section 2.2. The  $^1\text{H}$   $T_1$  value directly measured for the mobile  
 344 components (using  $T_2$ -filtered  $^1\text{H}$  NMR spectra) was  $T_1^{\text{mobile}} = 0.48$  s. On the other hand, the  $^1\text{H}$   $T_1$

345 value of the rigid components (measured indirectly via  $^{13}\text{C}$ -detected  $^1\text{H}$  saturation-recovery  
346 experiments, using  $^{13}\text{C}$  CP MAS NMR spectra) was  $T_1^{\text{rigid}} = 0.88$  s. This non-uniformity in the spin-  
347 lattice relaxation rates thus indicates that there is no fine mixing of the rigid and mobile components  
348 detected in the solid-state  $^1\text{H}$  and  $^{13}\text{C}$  NMR spectra of the coffee samples. This finding is consistent  
349 with the occurrence of the mobile and rigid components (associated with lipids and carbohydrates,  
350 respectively) in well-separated domains, as expected from the well-known morphological  
351 characteristics of the coffee beans, where oil-rich regions and cell walls exhibit sizes typically in the  
352 micron range (Kasai, Konishi, Iwai, & Maeda, 2006; Kanai et al., 2019).

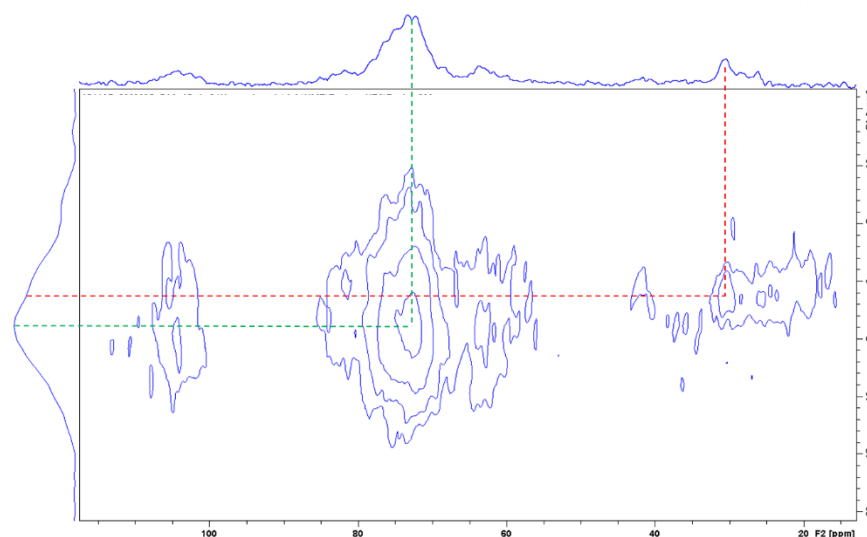
353 Similarly, experiments aimed at studying the possibility of  $^1\text{H}$  polarization transfer from the mobile  
354 components to the rigid ones were tried, revealing unsuccessful results. This type of experiments has  
355 been shown to be very useful to investigate the polarization transfer mechanism in lipid bilayers  
356 (Kumashiro et al., 1998), plant cell walls (White, Wang, Park, Cosgrove, & Hong, 2014) and starch  
357 hydrogels (Koev, Muñoz-García, Iuga, Khimyak, & Warren, 2020), for instance. In the case of the  
358  $T_2$ -filtered  $^1\text{H}$  NMR spectra of the coffee samples, if there were an effective interaction between the  
359  $^1\text{H}$  nuclei in the oil-rich and carbohydrate-rich phases (e.g., involving spin diffusion or chemical  
360 exchange), the signal due to the rigid components (removed with the use of the  $T_2$  filter) could be  
361 recovered after a mixing time; likewise, the insertion of a  $T_2$  filter followed by a spin diffusion interval  
362 previous to the contact time in the  $^{13}\text{C}$  CP MAS NMR experiments could reveal a recovery of the  $^{13}\text{C}$   
363 NMR signal due to the rigid components (White et al., 2014). The fail to observe such recovery either  
364 in the  $^1\text{H}$  or the  $^{13}\text{C}$  NMR experiments (even employing mixing times up to hundreds of ms) is a  
365 further corroboration of the scheme of two well-separated phases described above for the mobile and  
366 rigid components in the coffee samples.

367 This conclusion is further corroborated by the analysis of the 2D  $^1\text{H}$ - $^{13}\text{C}$  WISE results, illustrated in  
368 Fig. 6 for a representative coffee sample. In these experiments, the  $^1\text{H}$ - $^{13}\text{C}$  polarization transfer allows  
369 the correlation of  $^{13}\text{C}$  NMR spectra directly observed in the  $F_2$  dimension with the  $^1\text{H}$  NMR sideline  
370 spectra indirectly detected along the  $F_1$  dimension – with the latter being composed only of signals

371 due to  $^1\text{H}$  nuclei that are effective in cross-polarizing the  $^{13}\text{C}$  nuclei (Schmidt-Rohr et al., 1992). The  
372 first noteworthy point in the plot shown in Fig. 6 is the dissimilarity between the  $^1\text{H}$  ( $F_1$ ) projection  
373 of the 2D WISE spectra and the directly detected  $^1\text{H}$  NMR 1D spectra shown in Figs. 1 and 2. Whereas  
374 the 1D spectra are dominated by the narrow signals associated with lipids (mobile components), the  
375  $^1\text{H}$  ( $F_1$ ) projection of the 2D WISE spectra comprises a quite broad and featureless resonance, nearly  
376 matching the broad signal observed in Fig. 2, which was attributed to the  $^1\text{H}$  nuclei in rigid  
377 carbohydrate components. This finding is consistent with the ineffectiveness of the CP process for  
378 the highly mobile lipid groups, so the contributions due to the  $^1\text{H}$  nuclei in carbohydrates dominate  
379 the  $F_1$  projection of the WISE spectra. This result is similar to previous reports involving polymers  
380 (Schmidt-Rohr et al., 1992), cellulose (Ali, Apperley, Eley, Emsley & Harris, 1996), soil samples  
381 (Jäger, Schaumann & Bertmer, 2011) and porous carbon materials (Lopes et al., 2017).

382 Furthermore, the comparison between the plots in Fig. 6 and in Fig. 4 shows that, as expected, the  
383  $^{13}\text{C}$  ( $F_2$ ) projections of the 2D WISE spectra are quite similar to the  $^{13}\text{C}$  CP MAS NMR spectra, which  
384 are dominated by contributions due to the rigid carbohydrate moieties. There are clear correlations  
385 between the  $^{13}\text{C}$  signals at 66, 74 and 105 ppm and the maximum of the  $^1\text{H}$  ( $F_1$ ) projection around  
386 4.5 ppm – a chemical shift consistent with  $^1\text{H}$  nuclei in carbohydrates (Ali et al., 1996). This finding  
387 corroborates the interpretation given above about the origin of the broad signals observed in the  $^1\text{H}$   
388 NMR spectra recorded with no  $T_2$  filter (see Fig. 1). On the other hand, the narrow signals observed  
389 around 30 ppm in the  $^{13}\text{C}$  ( $F_2$ ) projection of the 2D WISE spectrum of Fig. 6 exhibits a correlation  
390 with a shoulder of the  $^1\text{H}$  ( $F_1$ ) projection at a lower chemical shift (*ca.* 1.0 ppm). This value is close  
391 to the shifts of the strong and narrow signals observed in the 1D  $^1\text{H}$  NMR spectra (see Figs. 1 and 2),  
392 attributed to  $\text{CH}_2$  groups in lipids; similarly, the chemical shift of 30 ppm corresponds to the narrow  
393 peaks observed in the  $^{13}\text{C}$  CP-SP MAS NMR spectra (Fig. 4). Thus, this correlation indicates the  
394 existence of residual dipolar couplings that allow the observation of the lipid signals (although with  
395 reduced intensity) in the 2D WISE spectra, evidencing that the high molecular mobility of these  
396 moieties does not completely preclude the polarization transfer from the  $^1\text{H}$  nuclei to the  $^{13}\text{C}$  nuclei.

397 It is clear, however, that this mobility causes a significant intensity reduction in the lipid signals, as  
398 already observed in the comparison between the CP and CP-SP spectra shown in Fig. 4. No  
399 correlation between the signals due to lipids and carbohydrates is detected in the 2D WISE spectra,  
400 reinforcing once more the scenario of two well-separated phases with marked distinct molecular  
401 mobilities for these chemical species in the coffee samples here investigated.



402

403 **Figure 6** – 2D WISE NMR spectrum recorded for the sample containing 100 wt. % Arabica coffee.

404 The dotted lines indicate the main correlations identified in the plot.

405

#### 406 **4. Conclusions**

407 Solid-state NMR spectroscopy with  $^1\text{H}$  and  $^{13}\text{C}$  as probe nuclei and employing a suite of distinct  
408 approaches (*e.g.*, CP and CP-SP methods for  $^{13}\text{C}$  NMR; use of  $T_2$  filter and selective measurements  
409 of  $T_1$  for  $^1\text{H}$  NMR; recording of 2D  $^1\text{H}$ - $^{13}\text{C}$  WISE spectra) has been shown in this work to be a  
410 powerful method for the characterization of roasted coffee samples at the molecular level. The use of  
411 these different approaches has allowed the detection of NMR signals originated from phases with  
412 marked distinct dynamics present in the heterogeneous structure of the material. The results were  
413 interpreted considering a scenario where lipids (high-mobility phase) and carbohydrates (rigid phase)  
414 contribute differently to the  $^1\text{H}$  and  $^{13}\text{C}$  NMR spectra. This scenario is thus consistent with the well-

415 known morphological characteristics of the coffee beans, containing well-separated oil-rich regions  
416 and carbohydrate-rich cell walls.

417 The potential of solid-state NMR spectroscopy to distinguish the contributions from Arabica and  
418 Robusta coffee variants in coffee blends was also demonstrated, illustrating the usefulness of this  
419 approach for screening and identification of counterfeit coffee products. As the  $^1\text{H}$  NMR spectra  
420 (especially when recorded with use of the  $T_2$  filter) are completely dominated by the lipid  
421 contributions and considering that the oil fraction is higher in the Arabica variety than in the Robusta  
422 one, specific  $^1\text{H}$  NMR signals (e.g., associated with diterpenes) can effectively be used as indicators  
423 of the amount of Arabica coffee in a mixture. The differences detected in the spectral regions  
424 corresponding to the signals due to these compounds evidence a clear distinction between the Arabica  
425 and Robusta contributions. These differences can then be analyzed with the help of chemometric  
426 multivariate methods, which would allow the establishment of analytical methods to detect the  
427 amounts of Arabica and Robusta varieties in coffee blends based on the solid-state NMR approach;  
428 this is certainly a promising way to expand this line of investigation in future work.

429 The solid-state NMR experiments here described are non-destructive, relatively fast and  
430 straightforward to implement in commercial NMR spectrometers equipped with conventional solid-  
431 state probes. Moreover, the coffee samples are analysed as received, with no need to dilute or obtain  
432 lipophilic extracts (as required in solution NMR experiments), which also avoids problems related to  
433 sample degradation. It is clear that further studies are required to establish these methods as useful  
434 analytical tools for coffee screening purposes, such as the evaluation of the consequences of the  
435 variability in the oil contents of Arabica coffee samples from different regions and the establishment  
436 of the limit of detection of Robusta coffee fraudulently mixed with Arabica coffee. On the other hand,  
437 the straightforward sample preparation for solid-state NMR experiments, the reproducibility of the  
438 obtained results over time, the relatively short analysis time (*ca.* 20 min for  $^1\text{H}$  and *ca.* 1.5 h for  $^{13}\text{C}$   
439 NMR experiments) and the promising correlations illustrated in this work stimulate the pursuing of

440 further in-depth investigations in this field, aiming applications of solid-state NMR as a practical  
441 method for the analysis of coffee products in the fields of food and forensic sciences.

442

#### 443 **ACKNOWLEDGEMENTS**

444 JCCF and WR acknowledge the support from Brazilian agencies CAPES (processes PE  
445 88881.178317/2018-01 and 23038.007083/2014-40), CNPq (grants 408001/2016-0 and  
446 310057/2020-5) and FAPES (process 280/2021).

447

#### 448 **REFERENCES**

449 Ali, M., Apperley, D. C., Eley, C. D., Emsley, A. M., & Harris, R. K. (1996). A solid-state NMR  
450 study of cellulose degradation. *Cellulose*, 3, 77-90. <https://doi.org/10.1007/BF02228792>

451 Aso, Y., Yoshioka, S., Miyazaki, T., Kawanishi, T., Tanaka, K., Kitamura, S., Takakura, A.,  
452 Hayashi, T., & Muranushi, N. (2007). Miscibility of nifedipine and hydrophilic polymers as  
453 measured by <sup>1</sup>H-NMR spin-lattice relaxation. *Chemical and Pharmaceutical Bulletin*, 55,  
454 1227-1231. <https://doi.org/10.1248/cpb.55.1227>

455 Bharti, S. K., & Roy, R. (2012). Quantitative <sup>1</sup>H NMR spectroscopy. *Trends in Analytical*  
456 *Chemistry*, 35, 5-26. <https://doi.org/10.1016/j.trac.2012.02.007>

457 Bosco, M., Toffanin, R., De Palo, D., Zatti, L., & Segre, A. (1999). High-resolution <sup>1</sup>H NMR  
458 investigation of coffee. *Journal of the Science of Food and Agriculture*, 79, 869-878.

459 [https://doi.org/10.1002/\(SICI\)1097-0010\(19990501\)79:6%3C869::AID-  
JSFA302%3E3.0.CO;2-6](https://doi.org/10.1002/(SICI)1097-0010(19990501)79:6%3C869::AID-<br/>460 JSFA302%3E3.0.CO;2-6)

461 Cano-Marquina, A., Tarín, J. J., & Cano, A. (2013). The impact of coffee on health. *Maturitas*, 75,  
462 7-21. <https://doi.org/10.1016/j.maturitas.2013.02.002>

463 Cipriano, D. F., Chinelatto Jr., L. S., Nascimento, S. A., Rezende, C. A., de Menezes, S. M. C., &

464 Freitas, J. C. C. (2020). Potential and limitations of  $^{13}\text{C}$  CP/MAS NMR spectroscopy to  
465 determine the lignin content of lignocellulosic feedstock. *Biomass and Bioenergy*, *142*, 105792.  
466 <https://doi.org/10.1016/j.biombioe.2020.105792>

467 Clauss, J., Schmidt-Rohr, K., & Spiess, H. W. (1993). Determination of domain sizes in  
468 heterogeneous polymers by solid-state NMR. *Acta Polymerica*, *44*, 1-17.  
469 <https://doi.org/10.1002/actp.1993.010440101>

470 Correia, R. M., Tosato, F., Domingos, E., Rodrigues, R. R. T., Aquino, L. F. M., Filgueiras, P. R.,  
471 Lacerda Jr., V., Romão, W. (2018). Portable near infrared spectroscopy applied to quality  
472 control of Brazilian coffee. *Talanta*, *176*, 59-68. <https://doi.org/10.1016/j.talanta.2017.08.009>

473 Courtier-Murias, D., Farooq, H., Longstaffe, J. G., Kelleher, B. P., Hart, K. M., Simpson, M. J., &  
474 Simpson, A. J. (2014). Cross polarization-single pulse/magic angle spinning (CPSP/MAS): A  
475 robust technique for routine soil analysis by solid-state NMR. *Geoderma*, *226-227*, 405-414.  
476 <http://dx.doi.org/10.1016/j.geoderma.2014.03.006>

477 D'Amelio, N., De Angelis, E., Navarini, L., Schievano, E., & Mammi, S. (2013) Green coffee oil  
478 analysis by high-resolution nuclear magnetic resonance spectroscopy. *Talanta*, *110*, 118-127.  
479 <https://doi.org/10.1016/j.talanta.2013.02.024>

480 Defernez, M., Wren, E., Watson, A. D., Gunning, Y., Colquhoun, I. J., Le Gall, G., Williamson, D.,  
481 & Kemsley, E. K. (2017). Low-field  $^1\text{H}$  NMR spectroscopy for distinguishing between arabica  
482 and robusta ground roast coffees. *Food Chemistry*, *216*, 106-113.  
483 <https://doi.org/10.1016/j.foodchem.2016.08.028>

484 Duan, P., Lamm, M. S., Yang, F., Xu, W., Skomski, D., Su, Y., & Schmidt-Rohr, K. (2020).  
485 Quantifying molecular mixing and heterogeneity in pharmaceutical dispersions at sub-100 nm  
486 resolution by spin diffusion NMR. *Molecular Pharmaceutics*, *17*, 3567-3580.  
487 <https://dx.doi.org/10.1021/acs.molpharmaceut.0c00592>

488 Esquivel, P., & Jiménez, V. M. (2012). Functional properties of coffee and coffee by-products.

489 *Food Research International*, 46(2), 488-495. <https://doi.org/10.1016/j.foodres.2011.05.028>

490 Finotello, C., Forzato, C., Gasparini, A., Mammi, S., Navarini, L., & Schievano, E. (2017). NMR  
491 quantification of 16-O-methylcafestol and kahweol in *Coffea canephora* var. robusta beans from  
492 different geographical origins. *Food Control*, 75, 62-69.

493 Gunning, Y., Defernez, M., Watson, A. D., Beadman, N., Colquhoun, I. J., Le Gall, G., Philo, M.,  
494 Garwood, H., Williamson, D., Davis, A. P., & Kemsley, E. K. (2018). 16-O-methylcafestol is  
495 present in ground roast Arabica coffees: Implications for authenticity testing. *Food Chemistry*,  
496 248, 52-60. <https://doi.org/10.1016/j.foodchem.2017.12.034>

497 Hong, E., Lee, S. Y., Jeong, J. Y., Park, J. M., Kim, B. H., Kwon, K., & Chun, H. S. (2017).  
498 Modern analytical methods for the detection of food fraud and adulteration by food category.  
499 *Journal of the Science of Food and Agriculture*, 97, 3877-3896.  
500 <https://doi.org/10.1002/jsfa.8364>

501 International Coffee Organization. Trade Statistics Tables. (2021).  
502 [http://www.ico.org/trade\\_statistics.asp](http://www.ico.org/trade_statistics.asp)> Accessed 28/10/2021.

503 Jäger, A., Schaumann, G. E., & Bertmer, M. (2011). Optimized NMR spectroscopic strategy to  
504 characterize water dynamics in soil samples. *Organic Geochemistry*, 42, 917-925.  
505 <http://dx.doi.org/10.1016/j.orggeochem.2011.03.021>

506 Kanai, N., Honda, T., Yoshihara, N., Oyama, T., Naito, A., Ueda, K., & Kawamura, I. (2020).  
507 Structural characterization of cellulose nanofibers isolated from spent coffee grounds and their  
508 composite films with poly(vinyl alcohol): a new non-wood source. *Cellulose*, 27, 5017-5028.  
509 <https://doi.org/10.1007/s10570-020-03113-w>

510 Kanai, N., Yoshihara, N., & Kawamura, I. (2019). Solid-state NMR characterization of  
511 triacylglycerol and polysaccharides in coffee beans. *Bioscience, Biotechnology, and*  
512 *Biochemistry*, 83, 803-809. <https://doi.org/10.1080/09168451.2019.1571899>

513 Kasai, N., Konishi, A., Iwai, K., & Maeda G. (2006). Efficient digestion and structural  
514 characteristics of cell walls of coffee beans. *Journal of Agricultural and Food Chemistry*, 54,  
515 6336-6342. <https://doi.org/10.1021/jf0609072>

516 Kemsley, E. K., Ruault, S., & Wilson, R. H. (1995). Discrimination between *Coffea arabica* and  
517 *Coffea canephora* variant robusta beans using infrared spectroscopy. *Food Chemistry*, 54, 321-  
518 326.

519 Koev, T. T., Muñoz-García, J. C., Iuga, D., Khimiyak, Y., & Warren, F. J. (2020). Structural  
520 heterogeneities in starch hydrogels. *Carbohydrate Polymers*, 249, 116384.  
521 <https://doi.org/10.1016/j.carbpol.2020.116834>

522 Kumashiro, K. K., Schmidt-Rohr, K., Murphy, O. J., Ouellette, K. L., Cramer, W. A., & Thompson,  
523 L. K. (1998). A novel tool for probing membrane protein structure: Solid-state NMR with  
524 proton spin diffusion and X-nucleus detection. *Journal of the American Chemical Society*, 120,  
525 5043-5051. <https://doi.org/10.1021/ja972655e>

526 Lesage, A. (2009). Recent advances in solid-state NMR spectroscopy of spin  $I = 1/2$  nuclei.  
527 *Physical Chemistry Chemical Physics*, 11, 6876-6891. <https://doi.org/10.1039/B907733M>

528 Lopes, T. R., Cipriano, D. F., Gonçalves, G. R., Honorato, H. A., Schettino Jr. M. A., Cunha, A. G.,  
529 Emmerich, F. G., & Freitas, J. C. C. (2017). Multinuclear magnetic resonance study on the  
530 occurrence of phosphorus in activated carbons prepared by chemical activation of  
531 lignocellulosic residues from the babassu production. *Journal of Environmental Chemical*  
532 *Engineering*, 5, 6016-6029. <https://doi.org/10.1016/j.jece.2017.11.028>

533 Low, J. H., Rahman, W. A. W. A., & Jamaluddin, J. (2015). Structural elucidation of tannins of  
534 spent coffee grounds by CP-MAS  $^{13}\text{C}$  NMR and MALDI-TOF MS. *Industrial Crops and*  
535 *Products*, 69, 456-461. <http://dx.doi.org/10.1016/j.indcrop.2015.03.001>

536 Mackenzie, K. J. D., & Smith, M. E. (2002). *Multinuclear solid-state NMR of inorganic materials*,  
537 Oxford: Pergamon.

538 Milani, M. A., Rossini, E. L., Catelani, T. A., Pezza, L., Toci, A. T., & Pezza, H. R. (2020).  
539 Authentication of roasted and ground coffee samples containing multiple adulterants using  
540 NMR and a chemometric approach. *Food Control*, *112*, 107104.  
541 <https://doi.org/10.1016/j.foodcont.2020.107104>

542 Monakhova, Y. B., Ruge, W., Kuballa, T., Ilse, M., Winkelmann, O., Diehl, B., Thomas, F., &  
543 Lachenmeier, D. W. (2015). Rapid approach to identify the presence of Arabica and Robusta  
544 species in coffee using <sup>1</sup>H NMR spectroscopy. *Food Chemistry*, *182*, 178-184.  
545 <https://doi.org/10.1016/j.foodchem.2015.02.132>

546 Nogueira, R. F., Boffo, E. F., Tavares, M. I. B., Moreira, L. A., Tavares, L. A., & Ferreira, A. G.  
547 (2011). The use of solid state NMR to evaluate the carbohydrates in commercial coffee  
548 granules. *Food and Nutrition Sciences*, *2*, 350-355. <https://doi:10.4236/fns.2011.24050>

549 Parker, T., Limer, E., Watson, A. D., Defernez, M., Williamson, D., & Kemsley, E. K. (2014) 60  
550 MHz <sup>1</sup>H NMR spectroscopy for the analysis of edible oils. *Trends in Analytical Chemistry* *57*,  
551 147-158. <https://doi.org/10.1016/j.trac.2014.02.006>

552 Rastrelli, F., Jha, S., & Mancin, F. 2009. Seeing through macromolecules: T<sub>2</sub>-filtered NMR for the  
553 purity assay of functionalized nanosystems and the screening of biofluids. *Journal of the*  
554 *American Chemical Society*, *131*, 14222-14224. <https://doi.org/10.1021/ja904737r>

555 Ribeiro, M. V. M., Boralle, N., Pezza, H. R., Pezza, L., & Toci, A. T. (2017). Authenticity of  
556 roasted coffee using <sup>1</sup>H NMR spectroscopy. *Journal of Food Composition and Analysis*, *57*,  
557 24-30. <https://doi.org/10.1016/j.jfca.2016.12.004>

558 Schmidt-Rohr, K., Clauss, J., & Spiess, H. W. (1992). Correlation of structure, mobility, and  
559 morphological information in heterogeneous polymer materials by two-dimensional wideline-  
560 separation NMR spectroscopy. *Macromolecules*, *25*, 3273-3277.  
561 <https://doi.org/10.1021/ma00038a037>

562 Sezer, B., Apaydin, H., Bilge, G., & Boyaci, I. H. (2018). *Coffee arabica* adulteration: Detection of

563 wheat, corn and chickpea. *Food Chemistry*, 264, 142-148.  
564 <https://doi.org/10.1016/j.foodchem.2018.05.037>

565 Shu, J., Li, P., Chen, Q., & Zhang, S. (2010). Quantitative measurement of polymer compositions  
566 by NMR spectroscopy: Targeting polymers with marked difference in phase mobility.  
567 *Macromolecules*, 43, 8993-8996. <https://doi.org/10.1021/ma101711f>

568 Speer, K., & Kölling-Speer, I. (2006) The lipid fraction of the coffee bean. *Brazilian Journal of*  
569 *Plant Physiology*, 18, 201-216. <https://doi.org/10.1590/S1677-04202006000100014>

570 Toci, A. T., Farah, A., Pezza, H. R., & Pezza, L. (2016). Coffee adulteration: More than two  
571 decades of research. *Critical Reviews in Analytical Chemistry*, 46(2), 83-92.  
572 <https://doi.org/10.1080/10408347.2014.966185>

573 Wei, F., Furihata, K., Koda, M., Hu, F., Kato, R., Miyakawa, T., & Tanokura, M. (2012). <sup>13</sup>C NMR-  
574 based metabolomics for the classification of green coffee beans according to variety and origin.  
575 *Journal of Agricultural and Food Chemistry*, 60, 10118-10125.

576 White, P. B., Wang, T., Park, Y. B., Cosgrove, D. J., & Hong, M. (2014). Water-polysaccharide  
577 interactions in the primary cell wall of *Arabidopsis thaliana* from polarization transfer solid-  
578 state NMR. *Journal of the American Chemical Society*, 136, 10399-10409.  
579 <https://doi.org/10.1021/ja504108h>